Published in final edited form as:

*Neurobiol Aging*. 2014 March ; 35(3): 449–459. doi:10.1016/j.neurobiolaging.2013.08.031.

# β-Amyloid Impairs the Regulation of NMDA Receptors by Glycogen Synthase Kinase 3

**Yulei Deng**[a,c], **Zhe Xiong**[c], **Paul Chen**[c], **Jing Wei**[b,c], **Shengdi Chen**[a,*], **Zhen Yan**[b,c,*]

[a]Department of Neurology and Institute of Neurology, Rui Jin Hospital, School of medicine, Shanghai Jiao Tong University, Shanghai, 200025, China.

[b]VA Western New York Healthcare System, 3495 Bailey Ave, Buffalo, NY, USA.

[c]Department of Physiology and Biophysics, State University of New York at Buffalo, School of Medicine and Biomedical Sciences, Buffalo, NY 14214, USA.

## Abstract

Accumulating evidence suggests that glycogen synthase kinase 3 (GSK-3) is a multifunctional kinase implicated in Alzheimer's disease (AD). However, the synaptic actions of GSK-3 in AD conditions are largely unknown. In this study, we examined the impact of GSK-3 on NMDA receptor (NMDAR) channels, the major mediator of synaptic plasticity. Application of GSK-3 inhibitors or knockdown of GSK-3 caused a significant reduction of NMDAR-mediated ionic and synaptic current in cortical neurons, while this effect of GSK-3 was impaired in cortical neurons treated with β-amyloid (Aβ) or from transgenic mice over-expressing mutant amyloid precursor protein (APP). GSK-3 activity was elevated by Aβ, and GSK-3 inhibitors failed to decrease the surface expression of NR1 and NR1/PSD-95 interaction in APP mice, which was associated with the diminished GSK-3 regulation of Rab5 activity that mediates NMDAR internalization. Consequently, GSK-3 inhibitor lost the capability of protecting neurons against NMDA-induced excitotoxicity in Aβ-treated neurons. These results have provided a novel mechanism underlying the involvement of GSK-3 in AD.

### Keywords

Alzheimer's disease; GSK-3; β-amyloid; NMDA receptor

Alzheimer's disease (AD) is a progressive neurodegenerative disorder with the pathological hallmarks of senile plaques and neurofibrillary tangles (LaFerla and Oddo, 2005). Senile plaques are composed of β-amyloid (Aβ), a peptide processed from the amyloid precursor protein (APP) (Masters et al., 1985, Jucker and Walker, 2011), whereas neurofibrillary tangles are mainly composed of the cytoskeleton protein tau in its hyperphosphorylated state

*Corresponding author at: Dr. Zhen Yan, Department of Physiology & Biophysics, State University of New York at Buffalo, Buffalo, NY 14214, USA. Tel.: +17168293058; fax: +17168292699. zhenyan@buffalo.edu, or Dr. Shengdi Chen, Department of Neurology & Institute of Neurology, Rui Jin Hospital, School of Medicine, Shanghai Jiao Tong University, Shanghai, 200025, China. chen_sd@medmail.com.cn.

Conflict of interest

None of the authors have actual or potential conflicts of interest. None of the authors' institution has contracts relating to this research. There is no other agreement of authors or their institutions that could be seen as involving a financial interest in this work.

(Grundke-Iqbal et al., 1986, Nussbaum et al., 2012). Glycogen synthase kinase 3 (GSK-3), which was initially identified as an enzyme that regulates glycogen synthesis in response to insulin (Welsh et al., 1996), has been implicated in AD because of its association with β-amyloid and tau (Hernández F, 2010). GSK-3 mediates Aβ-induced neuritic damage in AD, and GSK-3 inhibitors block the production and accumulation of Aβ peptides by interfering with APP cleavage (Phiel et al., 2003, White et al., 2006, DaRocha-Souto et al., 2012). Moreover, the tau protein, an important player in microtubule dynamics and axonal transport (Drubin and Kirschner, 1986, Ebneth et al., 1998), is regulated by GSK-3. GSK-3 promotes tau phosphorylation, reducing its interaction with microtubules (Wagner et al., 1996, Pooler et al., 2012), which could result in the destabilization of microtubule network (Alonso et al., 1997, Schmidt et al., 2012). Inhibition of GSK prevents the formation of tau aggregates and degeneration in a transgenic mouse model of AD (Noble et al., 2005). Thus, pharmacological inhibitors of GSK-3 have emerged as a potential drug target for the treatment of Alzheimer's disease and other neurodegenerative diseases (Meijer et al., 2004, Nunes et al., 2013).

In addition to β-amyloid and tau, the N-methyl-D-aspartate (NMDA)-type glutamate receptor (NMDAR), a central player in regulating synaptic plasticity, and learning & memory (Collingridge and Bliss, 1995, Rondi-Reig et al., 2001), is also implicated in AD. Memantine, a specific low- to moderate-affinity uncompetitive NMDAR antagonist has been approved by the FDA for treating moderate to severe AD. Overactivation of NMDA receptors causes neuronal dysfunction and death, presumably due to excess calcium influx through these channels and the over-accumulation of intracellular calcium (Michaelis, 1998). NMDA receptors can be directly activated by Aβ oligomers (Texido et al., 2011), and have been suggested to be a downstream effector of elevated Aβ and mediate the effects of tau in AD (Roberson et al., 2007).

GSK-3, the multifunctional serine/threonine kinase involved in many fundamental cell processes (Frame and Cohen, 2001, Hur and Zhou, 2010), also interacts with NMDA receptors. It has been found that strong stimulation of NMDA receptors induces the cleavage of GSK-3 by activated calpain (Goni-Oliver et al., 2007). Our previous study indicates that GSK-3 inhibitors down-regulate NMDAR-mediated current through increasing the NMDAR internalization (Chen et al., 2007). In this study, we sought to examine whether GSK-3 regulation of NMDARs goes awry in AD conditions. We found that Aβ led to the loss of NMDAR suppression by GSK-3 inhibitors, resulting in excitotoxicity reminiscent of AD.

## 1. Materials and Methods

### 1.1. Aβ oligomer preparation and an AD model

The procedure of Aβ oligomer preparation was similar to what was described before (Dahlgren et al., 2002; Gu et al., 2009; Liu et al., 2011). In brief, the $A\beta_{1–42}$ peptide (Tocris) was dissolved in hexafluoroisopropanol to 1 mM. Hexafluoroisopropanol was then removed under vacuum. The remaining peptide was then resuspended in DMSO to 5 mM and diluted in $H_2O$ to 0.1 mM. The oligomeric Aβ was formed by incubating at 4°C for 24 hr. APP transgenic mice carrying the Swedish mutation (K670N, M671L) (Hsiao et al., 1996) were purchased from Taconic (Germantown, NY). Eight-week-old transgenic males (on B6SJLF1

hybrid background) were bred with mature B6SJLF1 females. The genetic background of these mice is the same with this breeding scheme. Genotyping were performed by PCR according to the manufacturer's protocol.

### 1.2. Primary neuronal culture

Rat cortical cultures were prepared as previously described (Yuen et al., 2005, Gu et al., 2009). In brief, frontal cortex was dissected from E18 rat embryos, and cells were dissociated using trypsin and tituration through a Pasteur pipette. Neurons were plated on coverslips coated with poly-L-lysine in Dulbecco's modified Eagle's medium with 10% fetal calf serum at a density of $1\times10^5$ cells/$cm^2$. When neurons attached to the coverslips within 24 hr, the medium was changed to Neurobasal medium with B27 supplement (Invitrogen). Cytosine arabinoside (ARAC, 5 μM) was added at DIV 3 to stop glial proliferation.

### 1.3. Small interfering RNA

To suppress the expression of GSK-3 in cultured neurons, we used the small interfering RNA (siRNA), a potent agent for sequence-specific gene silencing. The GSK-3 siRNA oligonucleotide sequence selected from GSK-3α mRNA was: 5'-UUCUACUCCAGUGGUGAGAdTdT (sense); and from GSK-3β mRNA was: 5'-AUCUUUGGAGCCACU-GAUUdTdT (sense) (Phiel et al., 2003; Chen et al., 2007). The siRNA was synthesized (Ambion, Austin, TX) and cotransfected with enhanced GFP into cultured cortical neurons (DIV 14–16) using the Lipofectamine 2000 method. Two days after transfection, electrophysiological recordings were performed.

### 1.4. Whole-cell recordings in dissociated or cultured neurons

Acutely dissociated cortical pyramidal neurons from mice were prepared using procedures described previously (Wang et al., 2003). Recordings of whole-cell ion channel current in dissociated or cultured neurons used standard voltage-clamp techniques (Yuen et al., 2005). The internal solution consisted of 180 mM N-methyl-D-glucamine, 40 mM HEPES, 4 mM $MgCl_2$, 0.1 mM BAPTA, 12 mM phosphocreatine, 3 mM $Na_2ATP$, 0.5 mM $Na_2GTP$, and 0.1 mM leupeptin, pH 7.2–7.3, 265–270 mOsM. The external solution consisted of 127 mM NaCl, 20 mM CsCl, 10 mM HEPES, 1 mM $CaCl_2$, 5 mM $BaCl_2$, 12 mM glucose, 0.001 mM tetrodotoxin, and 0.02 mM glycine, pH 7.3–7.4, 300–305 mOsM. Recordings were obtained with an Axon Instruments 200B patch clamp amplifier that was controlled and monitored with an IBM PC running pCLAMP (version 8) with a DigiData 1320 series interface (Molecular Devices, Sunnyvale, CA). Electrode resistances were typically 2–4 MΩ in the bath. After seal rupture, series resistance (4–10 MΩ) was compensated (70–90%) and periodically monitored. The cell membrane potential was held at −60 mV. The application of NMDA (100 μM) evoked a partially desensitizing inward current that could be blocked by the NMDA receptor antagonist D-2-amino-5-phosphonovalerate (APV, 50 μM). NMDA was applied for 2 s every 30 s to minimize desensitization-induced decrease of current amplitude. Drugs were applied with a gravity-fed "sewer pipe" system. The array of application capillaries (approximately 150 μm internal diameter) was positioned a few hundred micrometers from the cell under study. Solution changes were affected by the SF-77B fast-step solution stimulus delivery device (Warner Instruments, Hamden, CT).

GSK-3 inhibitors SB216763 (Tocris, Ellisville, MO), 4-benzyl-2-methyl-1,2,4-thiadiazolidine-3,5-dione (TDZD, Calbiochem, San Diego, CA), and LiCl (Sigma-Aldrich, St. Louis, MO) were made up as concentrated stocks in DMSO or water and stored at −20°C. Stocks were thawed and diluted immediately before use.

### 1.5. Electrophysiological recordings in slices

To record NMDAR-mediated excitatory postsynaptic current in cortical slices, the whole-cell voltage-clamp recording technique was used (Wang et al., 2003, Yuen et al., 2005, 2012, Gu et al., 2009). Electrodes (5–9 MΩ) were filled with the following internal solution: 130 mM cesiummethanesulfonate, 10 mM CsCl, 4 mM NaCl, 10 mM HEPES, 1 mM $MgCl_2$, 5 mM EGTA, 2.2 mM QX-314, 12 mM phosphocreatine, 5 mM MgATP, 0.2 mM $Na_2GTP$, and 0.1 mM leupeptin, pH 7.2–7.3, 265–270 mOsM. The slice (300 μm) was placed in a perfusion chamber attached to the fixed-stage of an upright microscope (Olympus, Tokyo, Japan) and submerged in continuously flowing oxygenated artificial cerebrospinal fluid containing 6-cyano-2,3-dihydroxy-7-nitroquinoxaline (CNQX, 20 μM) and bicuculline (10 μM) to block α-amino-3-hydroxy-5-methyl-4-isoxazolepropionic acid (AMPA) receptors and $GABA_A$ receptors. Cells were visualized with a 40×water-immersion lens and illuminated with near infrared light, and the image was detected with an infrared-sensitive charge-coupled device camera. A Multiclamp 700A amplifier was used for these recordings. Tight seals (2–10 GΩ) from visualized pyramidal neurons were obtained by applying negative pressure. The membrane was disrupted with additional suction, and the whole-cell configuration was obtained. The access resistances ranged from 13 to 18 MΩ and were compensated 50–70%. Evoked currents were generated with a 50 μs pulse from a stimulation isolation unit controlled by an S48 pulse generator (Astro-Med, West Warwick, RI). A bipolar stimulating electrode (FHC) was positioned ~100 μm from the neuron under recording. Before stimulation, cells (voltage-clamped at −70 mV) were depolarized to +60 mV for 3 s to fully relieve the voltage-dependent $Mg^{2+}$ block of NMDAR channels.

### 1.6. Western blotting

After treatment, slices were homogenized in boiling 1% SDS, followed by centrifugation (13,000 × g, 20 min). The supernatant fractions were subjected to 7.5% SDS-polyacrylamidegels and transferred to nitrocellulose membranes. The blots were blocked with 5% nonfat dry milk for 1 hr at room temperature, followed by incubation with various primary antibodies including GSK-3α/β antibody (1:2000; Cell Signaling Technology), phospho-GSK-3α/β (Ser21/9) antibody (1:1000; Cell Signaling Technology) and phospho-GSK3α/β (Tyr279/216) antibody (1:1000; Millipore). The blots were exposed to the enhanced chemiluminescence substrate (Amersham Biosciences). Quantitation was obtained from densitometric measurements of immunoreactive bands on films.

### 1.7. Biochemical measurement of surface-expressed receptors

The surface NMDA receptors were detected as described previously (Gu et al., 2009; Yuen et al., 2012). In brief, after treatment, cortical slices were incubated with artificial cerebrospinal fluid (ACSF) containing 1 mg/ml sulfo-*N*-hydroxysuccinimide- LC-Biotin (Pierce Chemical Co., Rockford, IL) for 20 min on ice. The slices were then rinsed three times in Tris-buffered saline to quench the biotin reaction, followed by homogenization in

300 μl of modified radioimmunoprecipitation assay buffer (1% Triton X-100, 0.1% SDS, 0.5% deoxycholic acid, 50 mM $NaPO_4$, 150 mM NaCl, 2 mM EDTA, 50 mM NaF, 10 mM sodium pyrophosphate, 1 mM sodium orthovanadate, 1 mM phenylmethylsulfonyl fluoride, and 1 mg/ml leupeptin). The homogenates were centrifuged at 14,000 × *g* for 15 min at 4°C. Protein (15 μg) was removed to measure total NR1. For surface protein, 150 μg of protein was incubated with 100 μl of 50% Neutravidin Agarose (Pierce Chemical Co.) for 2 hr at 4°C, and bound proteins were resuspended in 25 μl of SDS sample buffer and boiled. Quantitative Western blots were performed on both total and biotinylated (surface) proteins using anti-NR1 (1:500; Neuromab).

### 1.8. Coimmunoprecipitation

After treatment, each slice was collected and homogenized in NP-40 lysis buffer (50 mM Tris, 1% deoxycholic acid, 10 mM EDTA, 10 mM EGTA, 1 mM phenylmethylsulfonyl fluoride, and 1 mg/ml leupeptin). Lysates were ultracentrifuged (200,000 × *g*) at 4°C for 1 hr. Supernatant fractions were incubated with anti-PSD95 (1:100; Affinity BioReagents, Golden, CO) or anti-Rab5 (20 μg, Santa Cruz Biotechnology, CA) for overnight at 4°C, followed by incubation with 50 μl of protein A/G plus agarose (Santa Cruz Biotechnology) for 2 hr at 4°C. Immunoprecipitates were washed three times with lysis buffer containing 0.2 M NaCl, then boiled in 2× SDS loading buffer for 5 min and separated on 7.5% SDS-polyacrylamide gels. Western blotting experiments were performed with antibodies against NR1 (1:500, Neuromab), PSD-95 (1:1000, Affinity BioReagents), Rabaptin-5 (1:500, Santa Cruz Biotechnology), or Rab5 (1:500, Santa Cruz Biotechnology).

### 1.9. Immunocytochemistry

Neuronal viability was evaluated with co-staining of propidium iodide (PI, to label apoptotic neurons) and microtubule associated protein-2 (MAP2) (to label survival neurons), as we previously described (Yuen et al., 2008). Cortical cultures (DIV14) were treated with NMDA (100 μM, 10 min), and returned to regular culture media. In some experiments, SB216763 (10 μM) was added 20 min before NMDA treatment. Some neurons were pretreated with $A\beta_{1–42}$ (1 μM) for 3 days before NMDA treatment. Twenty-four hours later NMDA treatment, cells were fixed with 4% paraformaldehyde for 20 min and permeabilized with 0.1% Triton X-100 for 20 min. After 1 hr incubation in 5% bovine serum albumin to block nonspecific staining, cells were incubated with anti-MAP2 (1:500; Chemicon) for 1 hr at room temperature. After washing, cells were incubated in a fluorescein isothiocyanate-conjugated secondary antibody (1:500; Invitrogen) for 2 hr at room temperature. After three washes in PBS, neurons were exposed to PI (4 μg/ml; Sigma) for 20 min at room temperature. After washing, coverslips were mounted on slides with VECTASHIELD mounting media (Vector Laboratories). The number of MAP2-positive neurons (survival neurons) and neurons showing shrunk and condensed nucleus in PI staining (apoptotic neurons) were counted and compared with control (untreated cultures). Each specimen was imaged under identical conditions and analyzed using identical parameters.

### 1.10. Data Analysis

Data analyses were performed with Clampfit (Molecular Devices) and Kaleidagraph (Abelbeck/Synergy Software, Reading, PA). Dose-response data were fitted with the

equation: $y = E_{max}/(1+(x/EC_{50})^h)$, where y is the effect, x is the dose, $E_{max}$ is the maximal effect, $EC_{50}$ is the dose that produces half-maximal effect, and h is the Hill coefficient. For analysis of statistical significance, Mann-Whitney U tests were performed to compare the current amplitudes in the presence or absence of GSK-3 inhibitors. Experiments with two groups were analyzed statistically using unpaired Student's *t*-tests. Experiments with more than two groups were subjected to one-way ANOVA, followed by *post hoc* Tukey tests. Cumulative data are shown as mean ± SEM.

## 2. Results

### 2.1. GSK-3 regulation of NMDAR currents is impaired in Aβ-treated neurons or APP transgenic mice

To determine the direct impact of Aβ on GSK-3 regulation of NMDARs, we pretreated cortical cultures with $Aβ_{1–42}$ oligomers (0.1 μM or 1 μM, >2 hr), which have already been aged and aggregated (Dahlgren et al., 2002; Gu et al., 2009; Liu et al., 2011). Exposure to different doses of $Aβ_{1–42}$ (0.1 μM or 1 μM, 2 hours) did not significantly alter the NMDA (100 μM)-elicited current density (pA/pF) in cultured cortical neurons (Fig. 1A, control: 31.5 ± 3.4, n=7; 0.1 μM Aβ: 30.1 ± 4.4, n = 6; 1 μM Aβ : 29.3 ± 3.0, n = 7, $p > 0.05$, ANOVA), consistent with our previous results (Gu et al., 2009). Application of SB 216763, a potent and selective GSK-3 inhibitor (Dash et al., 2011), caused a dose-dependent reduction of NMDAR current (Fig. 1B, n = 8 at each concentration), with the saturating effect at 10 μM, so this concentration was used in following studies.

To further confirm the involvement of GSK-3 in the regulation of NMDARs, we performed experiments in cortical neurons with GSK-3 knockdown. Compared to neurons (GFP+) transfected with a control siRNA, the NMDAR current density (pA/pF) was significantly smaller in neurons (GFP+) transfected with both GSK-3α and GSK-3β siRNAs (Fig. 1C, control siRNA: 37.7 ± 5.4, n = 5; GSK-3 KD: 24.5 ± 1.5, n = 7, $p < 0.01$, *t*-test), and was not subject to the regulation by SB216763 (10 μM, control siRNA: 20.6 ± 3.3%, n = 5, GSK-3 KD: 3.6 ± 0.7%, n = 9, $p < 0.001$, *t*-test, Fig. 1D). The knockdown effectiveness of GSK-3α and GSK-3β siRNAs in cortical cultures has been verified in our previous studies (Chen et al., 2007). These data suggest that inhibiting GSK-3 function or expression leads to the suppression of NMDAR current.

In $Aβ_{1–42}$-treated neurons, the reducing effect of SB216763 (10 μM) on NMDAR current was significantly diminished (Fig. 1E and 1F, control: 19.7 ± 2.7%, n = 8; 0.1 μM Aβ: 3.1 ± 1.6%, n = 7; 1 μM Aβ: 4.5 ± 1.3%, n = 7, $p < 0.001$, ANOVA). Another GSK-3 inhibitor LiCl (10 mM) also significantly reduced NMDAR current in control neurons, but not in $Aβ_{1–42}$-treated cells (Fig. 1G and 1H, control: 21.2 ± 5.6%, n = 6; 1 μM Aβ: 4.2 ± 2.6%, n = 7, $p < 0.001$, *t*-test).

Next, we examined the effect of GSK-3 on NMDAR-EPSC evoked by synaptic NMDAR activation in cortical slices. As shown in Fig. 2A and 2B, application of SB216763 (10 μM) produced a potent reduction of NMDAR-EPSC amplitudes, while in parallel measurements of Aβ-treated rat slices, the effect of SB216763 on NMDAR-EPSC was significantly attenuated (control: 47.7 ± 3.8%, n=7; Aβ-treated: 10.2 ± 2.0%, n = 7, $p < 0.001$, *t*-test).

To complement the results from *in vitro* short-term treatment of $A\beta_{1-42}$ oligomers, we also examined GSK-3 regulation of NMDARs in an established animal model for Alzheimer's disease, the APP transgenic mice carrying human APP695 with the double mutation K670N and M671L (Hsiao et al., 1996). The age-matched wild-type littermates were used as controls. As shown in Fig. 3A, SB216763 (10 μM) caused a significant reduction of NMDAR currents in cortical neurons isolated from wild-type mice, which was largely abolished in neurons from APP transgenic mice (Fig. 3B, WT: 19 ± 2%, n = 4; APP: 2 ± 1%, n = 7, $p < 0.001$, *t*-test). TDZD (10 μM), another GSK-3 inhibitor (Lipina et al., 2012), also reduced NMDAR-EPSC more significantly in neurons dissociated from WT than those from APP mice (Fig. 3C and 3D, WT: 22 ± 1%, n = 8; APP: 9 ± 1.4%, n = 10, $p < 0.001$, *t*-test).

We further examined the effect of GSK-3 on NMDAR-EPSC in slices from WT and APP mice. No significant difference was found in the basal NMDAR-EPSC amplitudes between WT and APP mice (Fig. 3E, WT: 292.1 ± 34.5 pA, n = 5; APP: 266.2 ± 25.3 pA, n = 5, $p > 0.05$, *t*-test), similar to what we found before (Gu et al., 2009). Application of SB216763 (10 μM) decreased the amplitude of NMDAR-EPSC in cortical neurons from WT mice, but not APP mice (Fig. 3F and 3G, WT: 54.3 ± 6.4%, n = 5; APP: 7.7 ± 1.9%, n = 4; $p < 0.001$, *t*-test). Taken together, these data provide the first evidence showing that the NMDAR response is regulated differently by GSK-3 in normal vs. AD-related conditions.

### 2.2. GSK-3 activity is elevated in Aβ-treated rat neurons and APP transgenic mice

Since GSK-3 inhibitors have lost the capability to regulate NMDARs in AD conditions, we speculate that it may be due to the altered GSK-3 activity. GSK-3α and GSK-3β are inactivated through phosphorylation of serine residues (Ser-21 for GSK-3α and Ser-9 for GSK-3β) on their N-terminal domain (Cross et al., 1995, Frame et al., 2001) and activated through phosphorylation of tyrosine residues (Tyr-279 for GSK-3α and Tyr-216 for GSK-3β) (Jope et al.,2007), so we used antibodys selective for Ser-21/9 or Tyr-279/216 **View All »**phosphorylated GSK-3 to determine the impact of Aβ oligomers on GSK-3 kinase activity.

As shown in Fig. 4A and 4B, treatment of cortical slices with Aβ (1 μM, 3-hr) markedly decreased the level of Ser-21/9 phosphorylated (inactive) GSK-3α/β (53.7 ± 8.9% of control, n = 4, $p < 0.01$, ANOVA) without changing the level of total GSK-3α/β, suggesting that Aβ treatment elevates the level of active GSK-3. Next, we examined Ser-21/9 phosphorylated (inactive) and Tyr-279/216 phosphorylated (active) GSK-3α/β in APP transgenic mice (12-month-old). As shown in Fig. 4C and 4D, compared to age-matched wild-type mice, the level of Ser-21/9 phosphorylated GSK-3α/β was significantly lower in cortical slices from APP mice (41.6 ± 7.8% of WT, n = 3, $p < 0.01$, *t*-test), and the level of Tyr-279/216 phosphorylated GSK-3α/β was significantly higher in cortical slices from APP mice (166.8 ± 16.3% of WT, n = 3, $p < 0.01$, t-test). These data suggest that GSK-3 kinase activity is increased in APP mice.

### 2.3. GSK-3 regulation of NMDAR surface expression and NR1/PSD-95 interaction is compromised in APP transgenic mice

To test whether the GSK-3 regulation of NMDA currents can be accounted for by the altered number of NMDA receptors on the cell membrane, we performed surface biotinylation experiments to measure levels of surface NR1 in cortical slices from WT vs. APP transgenic mice (10-month-old). Surface proteins were labeled with sulfo-NHS-LC-biotin, and then biotinylated surface proteins were separated from non-labeled intracellular proteins by reaction with Neutravidin beads. Surface and total proteins were subjected to eletrophoresis and probed with anti-NR1. As shown in Fig. 5A and 5B, SB216763 (10 μM, 15 min) treatment significantly decreased the level of surface NR1 in wild-type mice (64.3 ± 6.1% of WT control, $n = 9$, $p < 0.01$, ANOVA). In contrast, surface NR1 receptors was not changed by SB216763 treatment in APP mice (96.6 ± 6.4% of APP control, $n = 9$, $p > 0.05$, ANOVA). The basal level of surface NR1 in wild-type vs. APP mice was similar (APP: 97.2 ± 5.6% of WT, $n = 9$). These data suggest that the capability of GSK-3 inhibitors to reduce surface NMDARs was impaired in the AD model.

Since the effect of GSK-3 inhibitors on NMDAR currents and surface expression is dependent on the disruption of the interaction between the scaffolding protein PSD-95 and NMDAR subunits (Chen et al., 2007), we examined the impact of GSK-3 inhibitors on PSD-95/NMDAR association in the AD model. As shown in Fig. 6A and 6B, the binding between PSD-95 and NR1 was significantly reduced by SB216763 in WT mice (46 ± 6.5% of WT control, $n = 9$, $p < 0.01$, ANOVA), but not in APP transgenic mice (96.4 ± 2.2% of APP control, $n = 11$, $p > 0.05$, ANOVA). The inability of GSK-3 to regulate NR1/PSD-95 interaction may underlie the loss of GSK-3 regulation of NMDAR trafficking and function.

To further understand the potential mechanism underlying GSK-3 regulation of NMDA internalization, we examined the role of Rab5, a key mediator of protein transport from plasma membrane to early endosomes during endocytosis (Bucci et al., 1992; Brown et al., 2005). Our previous study has found that GSK-3 inhibitors induce the down-regulation of NMDAR current through increasing the Rab5-mediated and PSD-95-regulated NMDAR internalization in a clathrin/dynamin-dependent manner (Chen et al., 2007). We speculate that the GSK-3 regulation of Rab5-mediated endocytic pathways may be disrupted in APP mice. Since Rabaptin-5, a molecule identified as a Rab5-interacting protein, binds to the activate form of Rab5 (Vitale et al., 1998), we measured Rabaptin-5-bound Rab5 by co-immunoprecipitation experiments to indicate its activity level. As shown in Fig. 6C and 6D, SB216763 (10 μM, 15 min) treatment of cortical slices induced a significant increase of Rab5 activity in WT mice (173.4 ± 14.9% of WT control, $n = 3$, $p < 0.01$, ANOVA), but not in APP transgenic mice (95.2 ± 10.6% of APP control, $n = 3$, $p > 0.05$, ANOVA). It suggests that GSK-3 regulates NMDAR trafficking by changing Rab5 activity, which was impaired in the AD model.

### 2.4. The protective effect of GSK-3 inhibitor against NMDA-induced excitotoxicity is lost in Aβ-treated neurons

Because excessive $Ca^{2+}$ elevation by over-stimulation of NMDARs can cause excitotoxic neuronal death, the GSK-3 inhibitor-induced down-regulation of NMDAR function may

provide a neuroprotective effect against NMDAR-mediated excitotoxicity. To test this, we measured the effect of SB216763 on neuronal viability in cortical cultures treated with NMDA (100 μM, 10 min). To examine the effect of GSK-3 on excitotoxicity in AD conditions, we also pretreated some cortical cultures with $A\beta_{1-42}$ (1 μM) for 3 days before adding SB216763 and NMDA. Neurons were washed several times after NMDA treatment and kept in regular culture media. Twenty-four hours later, cultures were collected for immunocytochemical experiments. Apoptotic cell death was indicated by shrunk and condensed nucleus in PI staining (Ankarcrona et al., 1995, Bonfoco et al., 1995; Yuen et al., 2008), while surviving neurons were detected using the dendritic marker MAP2.

As shown in Fig. 7A, NMDA treatment induced remarkable apoptosis in cortical neurons, as indicated by significantly increased number of cells with shrunk and condensed nucleus in PI staining (control: 5.9 ± 1.4% apoptosis, n = 6, NMDA-treated: 81.2 ± 2.1% apoptosis, n = 6, Fig. 7C), and significantly decreased number of MAP2-positive neurons (18.7 ± 2.1% of control, n = 6, Fig. 7D). Note that NMDA-induced condensed nucleus PI staining occurred only in MAP2-negative neurons, but not in MAP2-positive neurons, suggesting that the MAP2-positive neurons were indeed healthy cells that remained alive. In the presence of SB216763 (10 μM, added 20 min before NMDA), neuronal death was decreased (Fig. 7A, 55.9 ± 1.2% apoptosis, n = 6, $p < 0.001$, ANOVA, compared to NMDA alone, Fig. 7C), and cell survival was increased (44.1 ± 1.2% of control, n = 6, $p < 0.001$, ANOVA, compared to NMDA alone, Fig. 7D). It suggests that GSK-3 inhibitor significantly attenuated NMDA-induced excitotoxicity and promoted cell survival in culture neurons.

Next, we examined the neuroprotective effect of GSK-3 inhibitor against NMDAR-mediated excitotoxicity in cultures pretreated with $A\beta_{1-42}$ (1 μM, added 3 days before NMDA treatment). No significant change on cell viability was observed in Aβ-treated cultures (Fig. 7B, control: 94.1 ± 1.4% survival, n = 6; Aβ: 93.1 ± 1.1% survival, n = 6, Fig. 7C), suggesting that Aβ (1 μM, 3 d) itself was not toxic to neurons. However, the protective effect of SB216763 (10 μM, added 20 min before NMDA treatment) against NMDA-induced excitotoxicity was abrogated by pretreatment with $A\beta_{1-42}$ (Fig. 7B, NMDA+Aβ: 83.0 ± 2.0% apoptosis, n = 6; SB+NMDA+Aβ: 80.0 ± 1.2% apoptosis, n = 6, Fig. 7C). It suggests that GSK-3 inhibitor lost the neuroprotective effect against NMDA-induced excitotoxicity, which may be due to the loss of its down-regulation of NMDAR currents in the presence of Aβ.

## 3. Discussion

A major challenge in the AD field is to determine the mechanism whereby synapses become dysfunctional in the disease, and many different synapse alterations have been found as a result of Aβ. For example, APP transgenic mice show an age-dependent reduction in hippocampal spine density, which occurs prior to plaque deposition (Lanz et al., 2003). Aβ treatment of cultured cortical neurons or Aβ accumulation in APP mice decreases PSD-95 protein levels and reduces the surface expression of AMPAR subunits (Roselli et al., 2005; Almeida et al., 2005). Our previous study has also demonstrated that CaMKII is reduced at the synapses by Aβ, which leads to the impairment of glutamatergic transmission due to the loss of synaptic AMPA receptors, but not NMDA receptors (Gu et al., 2009). Consistently,

another electrophysiological study has also reported that AMPAR current, but not NMDAR current, is reduced in 3.5-month-old APPswe/PS1dE9 mice (Shemer et al., 2006). Moreover, *in situ* hybridization finds no significant alterations on NMDAR mRNA in 4- and 15-month-old APP mice (Cha et al., 2001). In contrast, reduced amounts of surface NMDA receptors have been found in 12-day-old cultured neurons from APP mice, and decreased NMDAR currents by Aβ treatment (5 min) have been found in a subset of neurons (Snyder et al., 2005). The different biological properties of exogenous Aβ peptides or overexpressed mutant APP in different preparations may account for discrepancies in these studies. Synaptic loss of AMPA receptors is necessary and sufficient to produce loss of dendritic spines and synaptic NMDA responses (Hsieh et al., 2006), suggesting that the loss of synaptic AMPA receptors precedes other synaptic changes.

GSK-3, a multifunctional kinase that modulates many fundamental cell processes (Sereno et al., 2009, Hur and Zhou, 2010), has been linked to tau hyperphosphorylation (Alonso et al., 1997; Noble et al., 2005; Pooler et al., 2012; ) and Aβ production (Phiel et al., 2003, White et al., 2006, DaRocha-Souto et al., 2012) in AD. GSK-3 inhibition ameliorates plaque-related neuritic changes in double transgenic APP/tau mice, suggesting that Aβ-induced neuronal anatomical derangement is mediated, at least in part, by GSK-3 (DaRocha-Souto et al., 2012). Another study also suggests that GSK-3 is a player in Aβ pathology, because inhibition of GSK-3 restores lysosomal acidification that in turn enables Aβ clearance and mTOR reactivation, which facilitate amelioration in cognitive function (Avrahami et al., 2013).

The impact of Aβ on GSK-3 functions is largely unknown. Our previous study has found that NMDARs is an important target of GSK-3 at excitatory synapses (Chen et al., 2007). Given the importance of NMDARs in learning, memory and excitotoxicity, understanding how the regulation of NMDARs by GSK-3 goes awry in AD is very important for understanding the pathophysiology of this disease. In this study, we found that the reducing effect of GSK-3 inhibitors on NMDAR currents was impaired by $A\beta_{1–42}$ treatment and was attenuated in APP transgenic mice. In parallel with the loss of GSK-3 regulation of NMDAR function, the reducing effect of GSK-3 inhibitor on NR1 surface expression and NR1/PSD-95 interaction was also impaired in APP mice, which may be due to the dysregulation of Rab5-mediated NMDAR internalization. Consequently, GSK-3 inhibitor lost its capability to protect against NMDA-induced excitotoxicity in the presence of $A\beta_{1–42}$. It provides a new mechanism underlying the role of GSK-3 in AD.

GSK-3 is a serine/threonine kinase that was named after its involvement in glycogen metabolism (Embi et al., 1980). There were two closely related isoforms, GSK-3α and GSK-3β, which are expressed ubiquitously in mammalian tissues. GSK-3 is usually active in resting cells. Phosphorylation of certain GSK-3 residues can increase or decrease its ability to bind substrates (Jope et al., 2007). GSK-3 is a critical downstream element of the phosphoinositide 3-kinase/Akt pathway, and its activity can be inhibited by Akt-mediated phosphorylation at serine residues on its N-terminal domain (Cross et al., 1995). An increase in GSK-3 activity with age has been reported in the CNS of rats (Lee et al., 2006, Jimenez et al., 2011). Increased GSK-3 activity was also found in the temporal cortex of AD patients (DaRocha-Souto et al., 2012) and the mouse AD model carrying 5 mutations (5xFAD) that

develop massive cerebral Aβ loads (Avrahami et al., 2013). Consistently, we have detected the decreased $^{S9/21}$p-GSK-3 (inactive) and increased $^{Y279/216}$p-GSK-3 (active) in cultured cortical neurons exposed to oligomeric Aβ and in cortical slices of APP transgenic mice. Thus, GSK-3 is aberrantly activated by the presence of Aβ.

The synaptic localization of GSK-3 suggests that it might be involved in synaptic plasticity. In agreement with this, overactivation of GSK-3 has been found to inhibit the induction of hippocampal LTP (Hooper et al., 2007, Zhu et al., 2007). GSK-3 also mediates an interaction between NMDAR-dependent LTP and NMDAR-dependent LTD (Peineau et al., 2007). Overactivation of GSK-3β leads to the decreased expression of NMDAR subunits NR2A/B and the scaffolding protein PSD93 at synapses (Zhu et al., 2007). Our previous studies have shown that GSK-3 inhibitors suppress the endocytosis/internalization and function of NMDARs (Chen et al., 2007) and AMPARs (Wei et al., 2010), providing a direct mechanism for GSK-3 to regulate glutamatergic transmission.

While GSK-3 could regulate the production and degradation of β-amyloid peptides (Phiel et al., 2003, Ly et al., 2013), our present study suggests that the synaptic function of GSK-3 could also be affected by Aβ. GSK-3 inhibitors decrease NMDAR currents through increasing the Rab5-mediated NMDAR internalization in a clathrin/dynamin-dependent manner (Chen et al., 2007). The effects of GSK-3 on NMDAR trafficking and function are impaired by the presence of high levels of Aβ *in vitro* or *in vivo*, which may be attributed to the diminished regulation of Rab5 activity by GSK-3. Another possibility is that the putative GSK-3 substrate, such as the dynamin-like protein (Chen et al., 2000), has been changed by Aβ, which leads to the disturbance of NMDAR endocytosis. It suggests that NMDA receptors are under-suppressed by $PI_3$-kinase/Akt/GSK-3 signaling in AD conditions, which could contribute to the excitotoxicity caused by excessive calcium influx through overactive NMDAR channels.

GSK-3 has been implicated in apoptosis (Pap and Cooper, 1998, Guo et al., 2012), and *in vivo* overexpression of GSK-3 results in neurodegeneration (Lucas et al., 2001). Small-molecule inhibitors of GSK-3 were found to protect cultured neurons from death induced by reduced $PI_3$-kinase pathway activity (Cross et al., 2001). In this study, we have discovered that the protective action of GSK-3 inhibitor against NMDA-induced excitotoxicity is compromised in the presence of Aβ, which may be due to the diminished down-regulation of NMDA receptors by GSK-3 inhibitors in AD conditions. It is conceivable that dysregulation of NMDA receptors by altered GSK-3 signaling may be a key pathophysiological mechanism for neurodegenerative disorders.

## Acknowledgements

This work was supported by VA Merit Award (1I01BX001633) and NIH grants (MH084233, MH085774) to Z.Y., National Natural Science Foundation of China (81300932, 91332107) and Shanghai Natural Science Foundation (13ZR1425500) to S.C. We would like to thank Xiaoqing Chen for her excellent technical support.

## References


Almeida CG, Tampellini D, Takahashi RH, Greengard P, Lin MT, Snyder EM, Gouras GK, 2005 Beta-amyloid accumulation in APP mutant neurons reduces PSD-95 and GluR1 in synapses. Neurobiol. Dis. 20, 187–198. [PubMed: 16242627]

Alonso AD, Grundke-Iqbal I, Barra HS, Iqbal K, 1997 Abnormal phosphorylation of tau and the mechanism of Alzheimer neurofibrillary degeneration: sequestration of microtubule-associated proteins 1 and 2 and the disassembly of microtubules by the abnormal tau. Proc. Natl. Acad. Sci. U. S. A. 94, 298–303. [PubMed: 8990203]

Ankarcrona M, Dypbukt JM, Bonfoco E, Zhivotovsky B, Orrenius S, Lipton SA, Nicotera P, 1995 Glutamate-induced neuronal death: a succession of necrosis or apoptosis depending on mitochondrial function. Neuron. 15, 961–973. [PubMed: 7576644]

Avrahami L, Farfara D, Shaham-Kol M, Vassar R, Frenkel D, Eldar-Finkelman H, 2013 Inhibition of glycogen synthase kinase-3 ameliorates β-amyloid pathology and restores lysosomal acidification and mammalian target of rapamycin activity in the Alzheimer disease mouse model: in vivo and in vitro studies. J. Biol. Chem. 288, 1295–1306. [PubMed: 23155049]

Bonfoco E, Krainc D, Ankarcrona M, Nicotera P, Lipton SA, 1995 Apoptosis and necrosis: two distinct events induced, respectively, by mild and intense insults with N-methyl-D-aspartate or nitric oxide/superoxide in cortical cell cultures. Proc. Natl. Acad. Sci. U. S. A. 92, 7162–7166. [PubMed: 7638161]

Brown TC, Tran IC, Backos DS, Esteban JA, 2005 NMDA receptor-dependent activation of the small GTPase Rab5 drives the removal of synaptic AMPA receptors during hippocampal LTD. Neuron.45, 81–94. [PubMed: 15629704]

Bucci C, Parton RG, Mather IH, Stunnenberg H, Simons K, Hoflack B, Zerial M, 1992 The small GTPase rab5 functions as a regulatory factor in the early endocytic pathway. Cell. 70, 715–728. [PubMed: 1516130]

Cha JH, Farrell LA, Ahmed SF, Frey A, Hsiao-Ashe KK, Young AB, Penney JB, Locascio JJ, Hyman BT, Irizarry MC, 2001 Glutamate receptor dysregulation in the hippocampus of transgenic mice carrying mutated human amyloid precursor protein. Neurobiol. Dis. 8, 90–102. [PubMed: 11162243]

Chen CH, Hwang SL, Howng SL, Chou CK, Hong YR, 2000 Three rat brain alternative splicing dynamin-like protein variants: interaction with the glycogen synthase kinase 3beta and action as a substrate. Biochem. Biophys. Res. Commun. 268, 893–898 [PubMed: 10679301]

Chen P, Gu Z, Liu W, Yan Z, 2007 Glycogen synthase kinase 3 regulates N-methyl-D-aspartate receptor channel trafficking and function in cortical neurons. Mol. Pharmacol. 72, 40–51. [PubMed: 17400762]

Collingridge GL, Bliss TV, 1995 Memories of NMDA receptors and LTP. Trends. Neurosci. 18, 54–56. [PubMed: 7537406]

Cross DA, Alessi DR, Cohen P, Andjelkovich M, Hemmings BA, 1995 Inhibition of glycogen synthase kinase-3 by insulin mediated by protein kinase B. Nature. 378, 785–789. [PubMed: 8524413]

Cross DA, Culbert AA, Chalmers KA, Facci L, Skaper SD, Reith AD, 2001 Selective small-molecule inhibitors of glycogen synthase kinase-3 activity protect primary neurones from death. J Neurochem. 77, 94–102. [PubMed: 11279265]

Dahlgren KN, Manelli AM, Stine WB Jr., Baker LK, Krafft GA, LaDu MJ, 2002 Oligomeric and fibrillar species of amyloid-beta peptides differentially affect neuronal viability. J. Biol. Chem. 277, 32046–32053. [PubMed: 12058030]

DaRocha-Souto B, Coma M, Perez-Nievas BG, Scotton TC, Siao M, Sanchez-Ferrer P, Hashimoto T, Fan Z, Hudry E, Barroeta I, Sereno L, Rodriguez M, Sanchez MB, Hyman BT, Gomez-Isla T, 2012 Activation of glycogen synthase kinase-3 beta mediates beta-amyloid induced neuritic damage in Alzheimer's disease. Neurobiol. Dis. 45, 425–437. [PubMed: 21945540]

Dash PK, Johnson D, Clark J, Orsi SA, Zhang M, Zhao J, Grill RJ, Moore AN, Pati S, 2011 Involvement of the glycogen synthase kinase-3 signaling pathway in TBI pathology and neurocognitive outcome. PLoS. One. 6, e24648. [PubMed: 21935433]

Drubin DG, Kirschner MW, 1986 Tau protein function in living cells. J. Cell. Biol. 103, 2739–2746. [PubMed: 3098742]

Ebneth A, Godemann R, Stamer K, Illenberger S, Trinczek B, Mandelkow E, 1998 Overexpression of tau protein inhibits kinesin-dependent trafficking of vesicles, mitochondria, and endoplasmic reticulum: implications for Alzheimer's disease. J. Cell. Biol. 143, 777–794. [PubMed: 9813097]

Embi N, Rylatt DB, Cohen P, 1980 Glycogen synthase kinase-3 from rabbit skeletal muscle. Separation from cyclic-AMP-dependent protein kinase and phosphorylase kinase. Eur. J. Biochem. 107, 519–527. [PubMed: 6249596]

Frame S, Cohen P, Biondi RM, 2001 A common phosphate binding site explains the unique substrate specificity of GSK3 and its inactivation by phosphorylation. Mol. Cell. 7, 1321–1327. [PubMed: 11430833]

Frame S, Cohen P, 2001 GSK3 takes centre stage more than 20 years after its discovery. Biochem. J. 359, 1–16. [PubMed: 11563964]

Goni-Oliver P, Lucas JJ, Avila J, Hernandez F, 2007 N-terminal cleavage of GSK-3 by calpain: a new form of GSK-3 regulation. J. Biol. Chem. 282, 22406–22413. [PubMed: 17569662]

Grundke-Iqbal I, Iqbal K, Quinlan M, Tung YC, Zaidi MS, Wisniewski HM, 1986 Microtubule-associated protein tau. A component of Alzheimer paired helical filaments. J. Biol. Chem. 261, 6084–6089. [PubMed: 3084478]

Gu Z, Liu W, Yan Z, 2009 {beta}-Amyloid impairs AMPA receptor trafficking and function by reducing Ca2+/calmodulin-dependent protein kinase II synaptic distribution. J. Biol. Chem. 284, 10639–10649. [PubMed: 19240035]

Guo S, Som AT, Waeber C, Lo EH, 2012 Vascular neuroprotection via TrkB- and Akt-dependent cell survival signaling. J. Neurochem. 123, 58–64. [PubMed: 23050643]

Hernández F, Gómez de Barreda E, Fuster-Matanzo A, Lucas JJ, Avila J, 2010 GSK3: a possible link between beta amyloid peptide and tau protein. Exp. Neurol. 223, 322–325. [PubMed: 19782073]

Hooper C, Markevich V, Plattner F, Killick R, Schofield E, Engel T, Hernandez F, Anderton B, Rosenblum K, Bliss T, Cooke SF, Avila J, Lucas JJ, Giese KP, Stephenson J, Lovestone S, 2007 Glycogen synthase kinase-3 inhibition is integral to long-term potentiation. Eur. J. Neurosci. 25, 81–86. [PubMed: 17241269]

Hsiao K, Chapman P, Nilsen S, Eckman C, Harigaya Y, Younkin S, Yang F, Cole G, 1996 Correlative memory deficits, Abeta elevation, and amyloid plaques in transgenic mice. Science. 274, 99–102. [PubMed: 8810256]

Hsieh H, Boehm J, Sato C, Iwatsubo T, Tomita T, Sisodia S, Malinow R, 2006 AMPAR removal underlies Abeta-induced synaptic depression and dendritic spine loss. Neuron. 52, 831–843. [PubMed: 17145504]

Hur EM, Zhou FQ, 2010 GSK3 signalling in neural development. Nat. Rev. Neurosci. 11, 539–551. [PubMed: 20648061]

Jimenez S, Torres M, Vizuete M, Sanchez-Varo R, Sanchez-Mejias E, Trujillo-Estrada L, Carmona-Cuenca I, Caballero C, Ruano D, Gutierrez A, Vitorica J, 2011 Age-dependent accumulation of soluble amyloid beta (Abeta) oligomers reverses the neuroprotective effect of soluble amyloid precursor protein-alpha (sAPP(alpha)) by modulating phosphatidylinositol 3-kinase (PI3K)/Akt-GSK-3beta pathway in Alzheimer mouse model. J. Biol. Chem. 286, 18414–18425. [PubMed: 21460223]

Jope RS, Yuskaitis CJ, Beurel E, 2007 Glycogen synthase kinase-3 (GSK3): inflammation, diseases, and therapeutics. Neurochem. Res.32, 577–595. [PubMed: 16944320]

Jucker M, Walker LC, 2011 Pathogenic protein seeding in Alzheimer disease and other neurodegenerative disorders. Ann. Neurol. 70, 532–540. [PubMed: 22028219]

LaFerla FM, Oddo S, 2005 Alzheimer's disease: Abeta, tau and synaptic dysfunction. Trends. Mol. Med. 11, 170–176. [PubMed: 15823755]

Lanz TA, Carter DB, Merchant KM, 2003 Dendritic spine loss in the hippocampus of young PDAPP and Tg2576 mice and its prevention by the ApoE2 genotype. Neurobiol. Dis. 13, 246–253. [PubMed: 12901839]

Lee SJ, Chung YH, Joo KM, Lim HC, Jeon GS, Kim D, Lee WB, Kim YS, Cha CI, 2006 Age-related changes in glycogen synthase kinase 3beta (GSK3beta) immunoreactivity in the central nervous system of rats. Neurosci. Lett. 409, 134–139. [PubMed: 17046157]

Lipina TV, Wang M, Liu F, Roder JC, 2012 Synergistic interactions between PDE4B and GSK-3: DISC1 mutant mice. Neuropharmacology. 62, 1252–62. [PubMed: 21376063]

Liu W, Dou F, Feng J, Yan Z, 2011 RACK1 is involved in β-amyloid impairment of muscarinic regulation of GABAergic transmission. Neurobiol. Aging. 32, 1818–1826. [PubMed: 19954860]

Lucas JJ, Hernandez F, Gomez-Ramos P, Moran MA, Hen R, Avila J, 2001 Decreased nuclear beta-catenin, tau hyperphosphorylation and neurodegeneration in GSK-3beta conditional transgenic mice. EMBO. J. 20, 27–39. [PubMed: 11226152]

Ly PT, Wu Y, Zou H, Wang R, Zhou W, Kinoshita A, Zhang M, Yang Y, Cai F, Woodgett J, Song W, 2013 Inhibition of GSK3beta-mediated BACE1 expression reduces Alzheimer-associated phenotypes. J. Clin. Invest. 123, 224–235. [PubMed: 23202730]

Masters CL, Simms G, Weinman NA, Multhaup G, McDonald BL, Beyreuther K, 1985 Amyloid plaque core protein in Alzheimer disease and Down syndrome. Proc. Natl. Acad. Sci. U. S. A. 82, 4245–4249. [PubMed: 3159021]

Meijer L, Flajolet M, Greengard P, 2004 Pharmacological inhibitors of glycogen synthase kinase 3. Trends. Pharmacol. Sci. 25, 471–480. [PubMed: 15559249]

Michaelis EK, 1998 Molecular biology of glutamate receptors in the central nervous system and their role in excitotoxicity, oxidative stress and aging. Prog. Neurobiol. 54, 369–415. [PubMed: 9522394]

Noble W, Planel E, Zehr C, Olm V, Meyerson J, Suleman F, Gaynor K, Wang L, LaFrancois J, Feinstein B, Burns M, Krishnamurthy P, Wen Y, Bhat R, Lewis J, Dickson D, Duff K, 2005 Inhibition of glycogen synthase kinase-3 by lithium correlates with reduced tauopathy and degeneration in vivo. Proc. Natl. Acad. Sci. U. S. A. 102, 6990–6995. [PubMed: 15867159]

Nunes MA, Viel TA, Buck HS, 2013 Microdose lithium treatment stabilized cognitive impairment in patients with Alzheimer's disease. Curr. Alzheimer. Res. 10, 104–107. [PubMed: 22746245]

Nussbaum JM, Schilling S, Cynis H, Silva A, Swanson E, Wangsanut T, Tayler K, Wiltgen B, Hatami A, Ronicke R, Reymann K, Hutter-Paier B, Alexandru A, Jagla W, Graubner S, Glabe CG, Demuth HU, Bloom GS, 2012 Prion-like behaviour and tau-dependent cytotoxicity of pyroglutamylated amyloid-beta. Nature. 485, 651–655. [PubMed: 22660329]

Pap M, Cooper GM, 1998 Role of glycogen synthase kinase-3 in the phosphatidylinositol 3-Kinase/Akt cell survival pathway. J. Biol. Chem. 273, 19929–19932. [PubMed: 9685326]

Peineau S, Taghibiglou C, Bradley C, Wong TP, Liu L, Lu J, Lo E, Wu D, Saule E, Bouschet T, Matthews P, Isaac JT, Bortolotto ZA, Wang YT, Collingridge GL, 2007 LTP inhibits LTD in the hippocampus via regulation of GSK3beta. Neuron. 53, 703–717. [PubMed: 17329210]

Phiel CJ, Wilson CA, Lee VM, Klein PS, 2003 GSK-3alpha regulates production of Alzheimer's disease amyloid-beta peptides. Nature. 423, 435–439. [PubMed: 12761548]

Pooler AM, Usardi A, Evans CJ, Philpott KL, Noble W, Hanger DP, 2012 Dynamic association of tau with neuronal membranes is regulated by phosphorylation. Neurobiol. Aging. 33, e427–438.

Roberson ED, Scearce-Levie K, Palop JJ, Yan F, Cheng IH, Wu T, Gerstein H, Yu GQ, Mucke L, 2007 Reducing endogenous tau ameliorates amyloid beta-induced deficits in an Alzheimer's disease mouse model. Science. 316, 750–754. [PubMed: 17478722]

Rondi-Reig L, Libbey M, Eichenbaum H, Tonegawa S, 2001 CA1-specific N-methyl-D-aspartate receptor knockout mice are deficient in solving a nonspatial transverse patterning task. Proc. Natl. Acad. Sci. U. S. A. 98, 3543–3548. [PubMed: 11248114]

Roselli F, Tirard M, Lu J, Hutzler P, Lamberti P, Livrea P, Morabito M, Almeida OF, 2005 Soluble beta-amyloid1–40 induces NMDA-dependent degradation of postsynaptic density-95 at glutamatergic synapses. J. Neurosci. 25, 11061–11070. [PubMed: 16319306]

Schmidt N, Basu S, Sladecek S, Gatti S, van Haren J, Treves S, Pielage J, Galjart N, Brenner HR, 2012 Agrin regulates CLASP2-mediated capture of microtubules at the neuromuscular junction synaptic membrane. J. Cell. Biol. 198, 421–437. [PubMed: 22851317]

Sereno L, Coma M, Rodriguez M, Sanchez-Ferrer P, Sanchez MB, Gich I, Agullo JM, Perez M, Avila J, Guardia-Laguarta C, Clarimon J, Lleo A, Gomez-Isla T, 2009 A novel GSK-3beta inhibitor

reduces Alzheimer's pathology and rescues neuronal loss in vivo. Neurobiol. Dis. 35, 359–367. [PubMed: 19523516]

Shemer I, Holmgren C, Min R, Fülöp L, Zilberter M, Sousa KM, Farkas T, Härtig W, Penke B, Burnashev N, Tanila H, Zilberter Y, Harkany T, 2006 Non-fibrillar beta-amyloid abates spike-timing-dependent synaptic potentiation at excitatory synapses in layer 2/3 of the neocortex by targeting postsynaptic AMPA receptors. Eur. J. Neurosci. 23, 2035–2047. [PubMed: 16630051]

Snyder EM, Nong Y, Almeida CG, Paul S, Moran T, Choi EY, Nairn AC, Salter MW, Lombroso PJ, Gouras GK, Greengard P, 2005 Regulation of NMDA receptor trafficking by amyloid-beta. Nat. Neurosci. 8, 1051–1058. [PubMed: 16025111]

Texido L, Martin-Satue M, Alberdi E, Solsona C, Matute C, 2011 Amyloid beta peptide oligomers directly activate NMDA receptors. Cell. calcium. 49, 184–190. [PubMed: 21349580]

Vitale G, Rybin V, Christoforidis S, Thornqvist P, McCaffrey M, Stenmark H, Zerial M, 1998 Distinct Rab-binding domains mediate the interaction of Rabaptin-5 with GTP-bound Rab4 and Rab5. EMBO. J. 17, 1941–1951. [PubMed: 9524117]

Wagner U, Utton M, Gallo JM, Miller CC, 1996 Cellular phosphorylation of tau by GSK-3 beta influences tau binding to microtubules and microtubule organisation. J. Cell. Sci. 109, 1537–1543. [PubMed: 8799840]

Wang X, Zhong P, Gu Z, Yan Z, 2003 Regulation of NMDA receptors by dopamine D4 signaling in prefrontal cortex. J. Neurosci. 23, 9852–9861. [PubMed: 14586014]

Wei J, Liu W, Yan Z, 2010 Regulation of AMPA receptor trafficking and function by glycogen synthase kinase 3. J. Biol. Chem. 285, 26369–26376. [PubMed: 20584904]

Welsh GI, Wilson C, Proud CG, 1996 GSK3: a SHAGGY frog story. Trends. Cell. Biol. 6, 274–279. [PubMed: 15157454]

White AR, Du T, Laughton KM, Volitakis I, Sharples RA, Xilinas ME, Hoke DE, Holsinger RM, Evin G, Cherny RA, Hill AF, Barnham KJ, Li QX, Bush AI, Masters CL, 2006 Degradation of the Alzheimer disease amyloid beta-peptide by metal-dependent up-regulation of metalloprotease activity. J. Biol. Chem. 281, 17670–17680. [PubMed: 16648635]

Yuen EY, Jiang Q, Chen P, Gu Z, Feng J, Yan Z, 2005 Serotonin 5-HT1A receptors regulate NMDA receptor channels through a microtubule-dependent mechanism. J. Neurosci. 25, 5488–5501. [PubMed: 15944377]

Yuen EY, Ren Y, Yan Z, 2008 PSD-95 and calcineurin control the sensitivity of NMDA receptors to calpain cleavage in cortical neurons. Mol. Pharmacol. 74, 360–370. [PubMed: 18445709]

Yuen EY, Wei J, Liu W, Zhong P, Li X, Yan Z, 2012 Repeated stress causes cognitive impairment by suppressing glutamate receptor expression and function in prefrontal cortex. Neuron 73, 962–977. [PubMed: 22405206]

Zhu LQ, Wang SH, Liu D, Yin YY, Tian Q, Wang XC, Wang Q, Chen JG, Wang JZ, 2007 Activation of glycogen synthase kinase-3 inhibits long-term potentiation with synapse-associated impairments. J. Neurosci. 27, 12211–12220. [PubMed: 17989287]

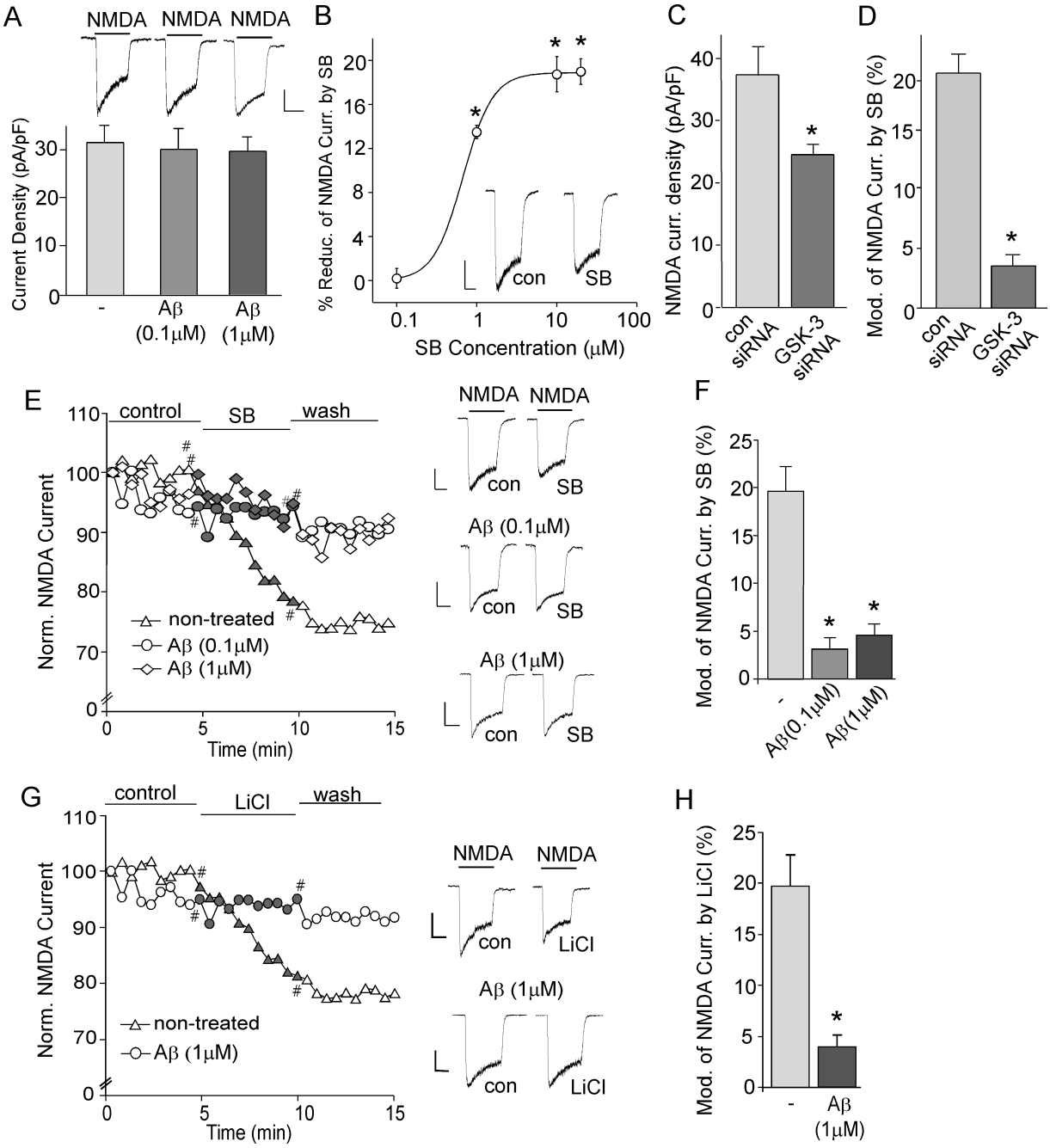


**Fig. 1. GSK-3 inhibitors fail to suppress NMDAR-mediated ionic currents in Aβ-treated neurons.**

**A**, Cumulative data showing the average NMDAR current densities in cultured cortical neurons untreated (control) or treated with $A\beta_{1-42}$ (0.1 μM or 1 μM, 2-hr). Inset: Representative current traces. Scale bar: 250 pA, 1 sec. **B,** Dose-response data showing the percentage reduction of NMDAR currents by different concentrations of SB216763. *: $p < 0.01$, Mann-Whitney U tests. Inset: Representative current traces. Scale bar, 250 pA, 1 sec. ANOVA. **C,** Cumulative data of NMDAR current densities in cultured cortical neurons transfected with GSK-3α and GSK-3β siRNAs or a scrambled control siRNA. *: $p < 0.01$, *t*-test. **D**, Cumulative data showing the percentage reduction of NMDAR currents by

SB216763 (10 μM) in neurons transfected with GSK-3α and GSK-3β siRNAs or a scrambled control siRNA. *: $p < 0.001$, *t*-test. **E, G**, Plot of normalized peak NMDAR current showing the effect of GSK-3 inhibitor SB216763 (10 μM, E) or LiCl (10 mM, G) in cultured cortical neurons treated without or with $A\beta_{1–42}$ (0.1 μM or 1 μM). Representative current traces taken from time points denoted by # are also shown. Scale bars: 250 pA, 1 sec. **F, H**, Cumulative data showing the percentage reduction of NMDAR current by SB216763 or LiCl in control vs. Aβ-treated cultures. *: $p < 0.001$, ANOVA (F); *: $p < 0.001$, *t*-test (H).

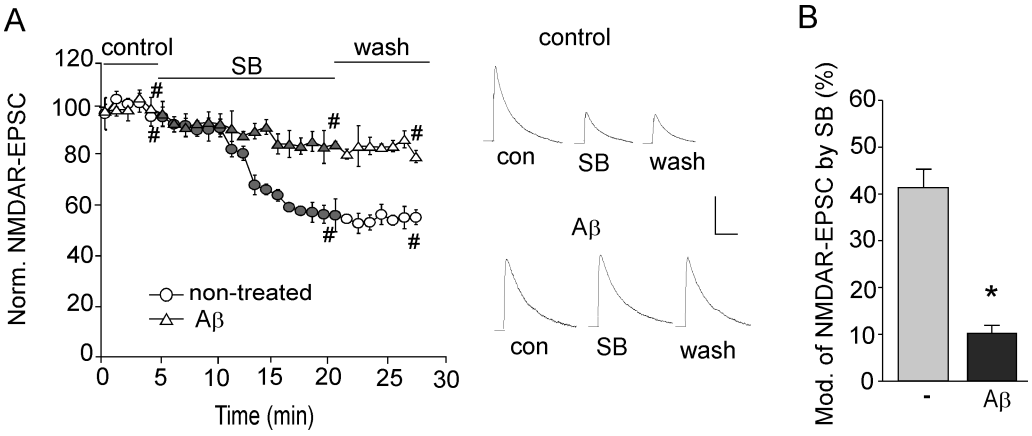


**Fig. 2. GSK-3 inhibitors fail to suppress NMDAR-mediated synaptic currents in Aβ-treated slices.**

**A**, Plot of normalized peak NMDAR-EPSC showing the effect of SB216763 (10 μM) in control vs. Aβ (1 μM)-treated rat cortical slices. Representative NMDAR-EPSC traces taken from time points denoted by # are also shown. Scale bars, 100 pA, 200 ms. **B**, Cumulative data showing the percentage reduction of NMDAR-EPSC by SB216763 in control vs. Aβ-treated slices. *: $p < 0.001$, *t*-test.

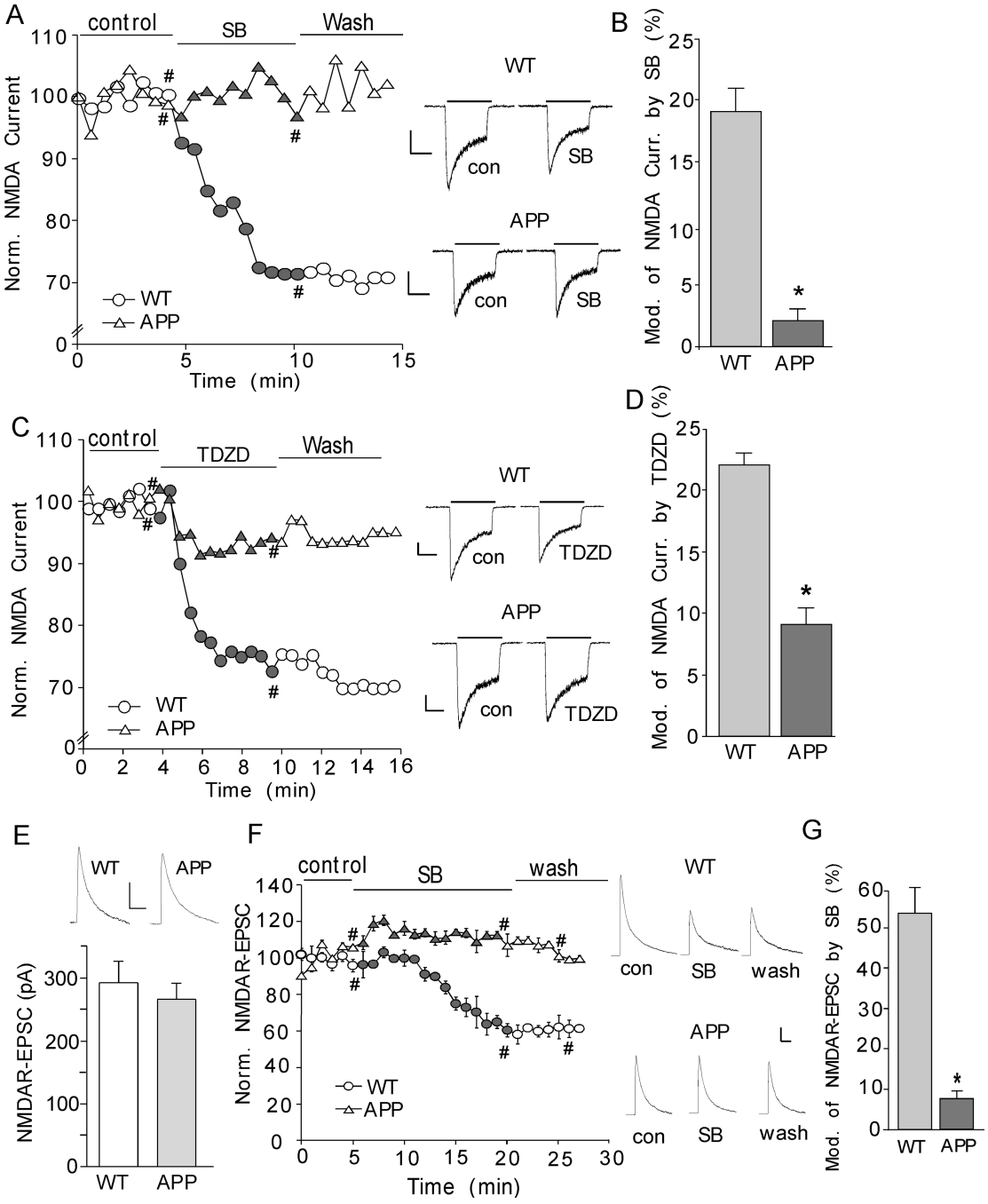


**Fig. 3. GSK-3 inhibitors fail to suppress NMDAR currents in APP transgenic mice.**

**A, C,** Plot of normalized peak NMDAR current showing the effect of the GSK-3 inhibitor SB216763 (10 μM, A) or TDZD (10 μM, C) in acutely dissociated cortical neurons from WT vs. APP transgenic mice. Representative current traces taken from time points denoted by # are also shown. Scale bars: 250 pA, 1 sec. **B, D,** Cumulative data showing the percentage reduction of NMDAR current by SB216763 or TDZD in WT vs. APP mice. *: $p < 0.001$, *t*-test. **E,** Cumulative data showing the average NMDAR-EPSC amplitudes in prefrontal cortical pyramidal neurons from WT and APP mice. Inset: Representative

NMDAR-EPSC traces. Scale bars, 100 pA, 200 ms. **F**, Plot of normalized NMDAR-EPSC showing the effect of SB216763 (10 μM) in cortical slices from WT vs. APP mice. Representative NMDAR-EPSC traces taken from time points denoted by # are also shown. Scale bars, 100 pA, 200 ms. **G**, Cumulative data showing the percentage reduction of NMDAR-EPSC by SB216763 in WT or APP mice. *: $p < 0.001$, *t*-test.

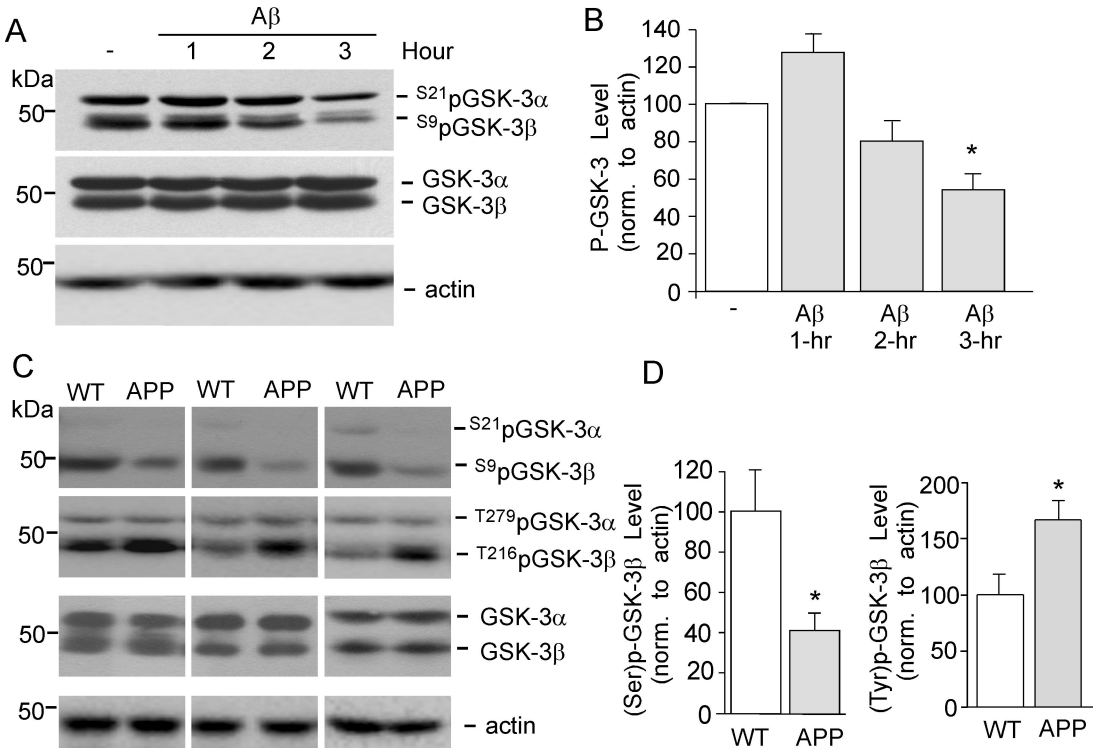


**Fig. 4. GSK-3 activity is increased in Aβ-treated neurons and APP transgenic mice.**

**A, B,** Representative Western blotting and quantitative analysis showing the effect of $A\beta_{1-42}$ treatment (1 μM, 1–3 hrs) on Ser-21/9 phosphorylated (inactive) GSK-3α/β, Tyr-279/216 phosphorylated (active) GSK-3α/β and total GSK-3α/β in cortical slices. The actin blots are shown below. *: $p < 0.01$, ANOVA. **C, D,** Representative Western blotting showing Ser-21/9 phosphorylated GSK-3α/β, Try-279/216 phosphorylated GSK-3α/β and total GSK-3α/β in cortical slices from WT vs. APP transgenic mice. The actin blots are shown below. *: $p < 0.01$, *t*-test.

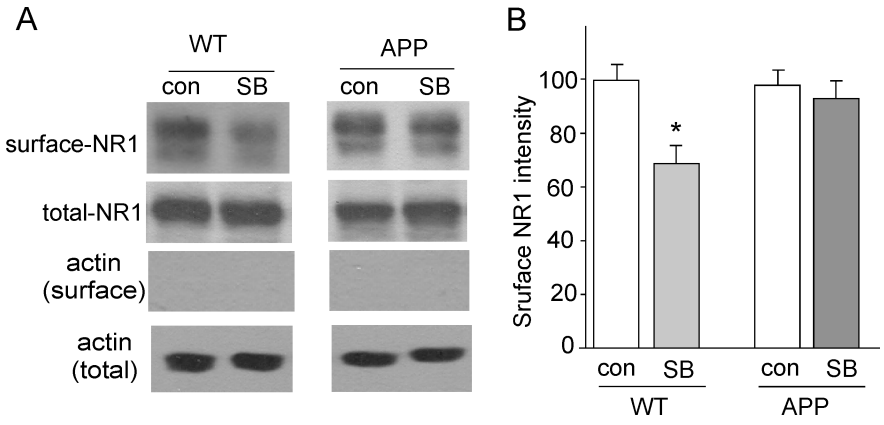


**Fig. 5. GSK-3 inhibitor fails to reduce the level of surface NR1 subunit in APP mice.**

**A,** Immunoblots of the surface and total NR1 subunit in cortical slices treated without or with SB216763 (10 μM, 15 min) from WT and APP mice. Actin was used as a control. **B**, Quantitation of surface NR1 subunit expression with various treatments. *: $p < 0.01$, ANOVA.

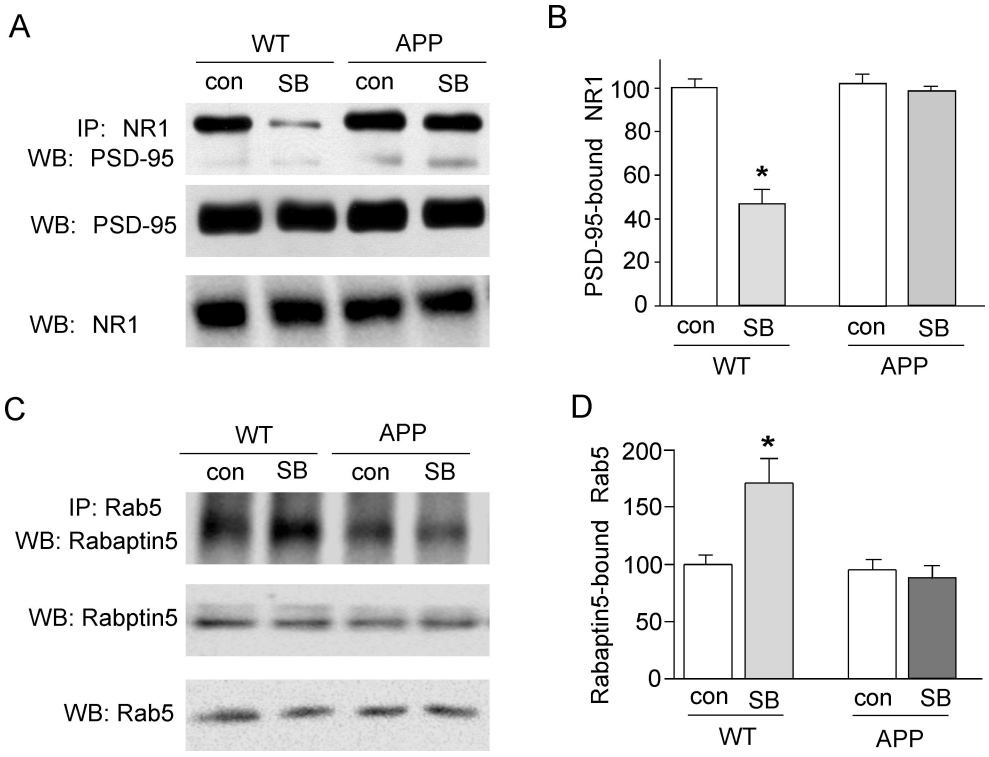


**Fig. 6. GSK-3 inhibitor fails to alter NMDAR-PSD-95 interaction and Rab5 activity in APP transgenic mice.**

**A,** Co-immuoprecipitation blots showing the association of NR1 with PSD-95 in the absence or presence of SB216763 (10 μM, 15 min) in cortical lysates from WT vs. APP mice. The blots of total PSD-95 and NR1 are shown below. **B,** Cumulative data showing the percent reduction of the binding between NR1 and PSD-95 by SB216763 in APP vs. WT mice. *: $p < 0.01$, ANOVA. **C,** Co-immuoprecipitation blots showing the association of Rab5 with Rabaptin-5 in the absence or presence of SB216763 (10 μM, 15 min) in cortical lysates from WT vs. APP mice. The blots of total Rab5 and Rabaptin-5 are shown below. **D,** Cumulative data showing the percent increase of the Rabaptin-5-bound Rab5 (active) by SB216763 in WT vs. APP mice. *: $p < 0.01$, ANOVA.

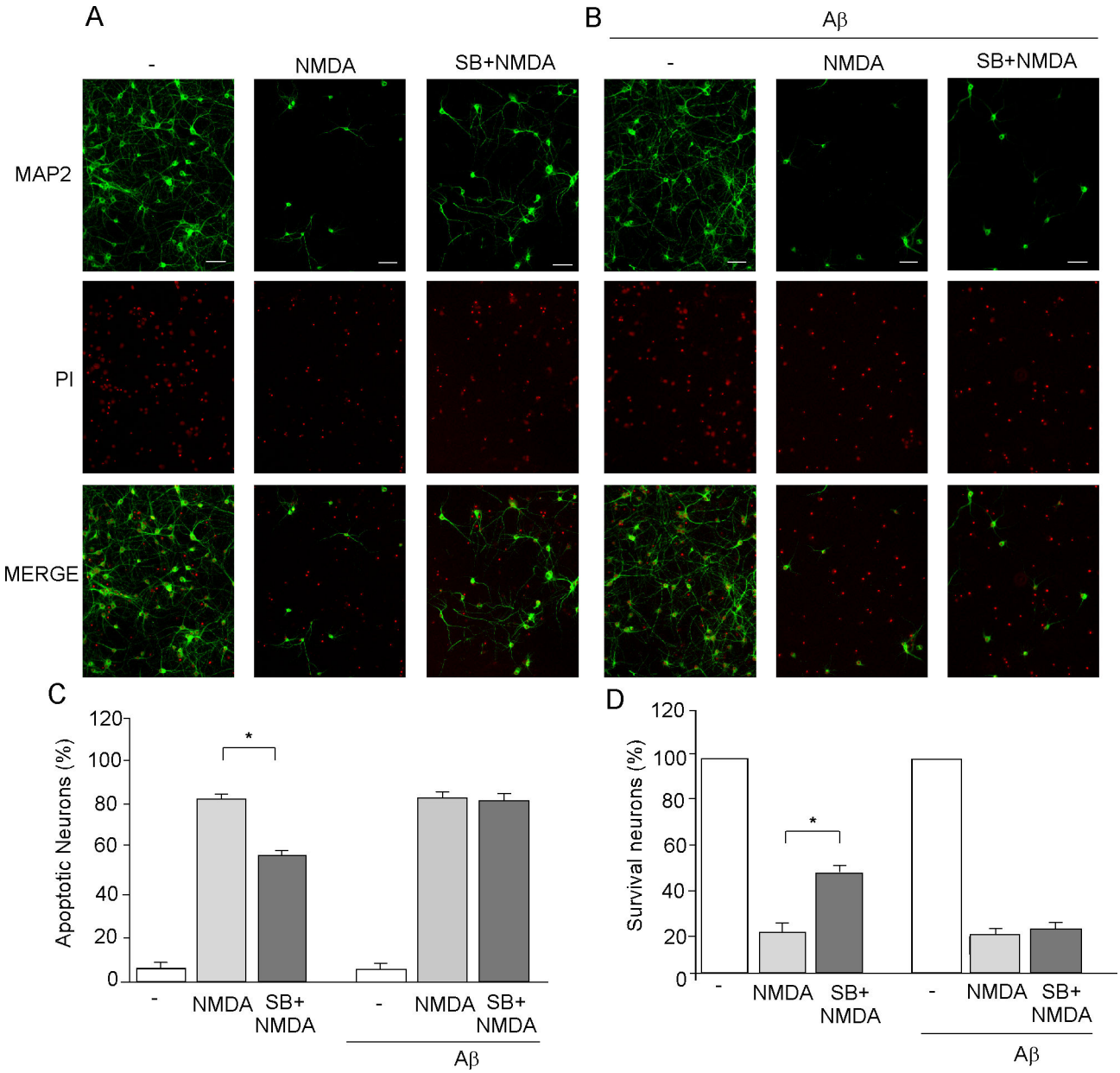


**Fig. 7. GSK-3 inhibitor fails to protect against NMDA-induced excitotoxicity in Aβ-treated neurons.**

**A, B**, Immunocytochemical images showing the co-staining of MAP2 (green) and propidium iodide (PI, red) in cortical cultures (A: control, B: pretreated with 1 μM Aβ for 3 days) treated without (−) or with NMDA (100 μM, 10 min) in the absence or presence of SB216763 (10 μM, added 20 min before NMDA). Scale bars: 100 μm. Apoptotic neurons were indicated by shrunk and condensed nucleus in PI staining. Survival neurons were positive for MAP2 staining. **C, D**, Cumulative data showing the percentage of apoptotic neurons (**C**) or survival neurons (**D**) under various treatments. *: $p < 0.001$, ANOVA.